Phospholipid interactions in model membrane systems

I. Experiments on monolayers

James Mingins,* Dirk Stigter,‡ and Ken A. Dill‡

*AFRC Institute of Food Research, Norwich Laboratory, Norwich, NR4 7UA, United Kingdom; and ‡Department of Pharmaceutical Chemistry, University of California, San Francisco, California 94143, USA

ABSTRACT We study the lateral headgroup interactions among phosphatidylcholine (PC) molecules and among phosphatidylethanolamine (PE) molecules in monolayers and extend our previous models. In this paper, we present an extensive set of pressure-area isotherms and surface potential experiments on monolayers of phospholipids ranging from 14 to 22 carbons in length at the *n*-heptane/water interface, over a wide range of temperature, salt concentration, and pH on the acid side. The pressure data presented here are a considerable extension of previous data (1) to higher surface densities, comprehensively checked for monolayer loss, and include new data on PE molecules. We explore surface densities ranging from extremely low to intermediate, near to the main phase transition, in which range the surface pressures and potentials are found to be independent of the chain length. Thus, these data bear directly on the headgroup interactions. These interactions are observed to be independent of ionic strength. PC and PE molecules differ strongly in two respects: (*a*) the lateral repulsion among PC molecules is much stronger than for PE, and (*b*) the lateral repulsion among PC molecules increases strongly with temperature whereas PE interactions are almost independent of temperature. Similarly, the surface potential for PC is found to increase with temperature whereas for PE it does not. In this and the following paper we show that these data from dilute to semidilute monolayers are consistent with a theoretical model that predicts that, independent of coverage, for PC the P^-N^+ dipole is oriented slightly into the oil phase because of the hydrophobicity of the methyl groups, increasingly so with temperature, whereas for PE the P^-N^+ dipole is directed into the water phase.

INTRODUCTION

The phosphatidylcholines (PC's) and phosphatidylethanolamines (PE's) are the two major classes of neutral phospholipids found in the lipid fraction of many cell membranes. It has been found that the physical properties of bilayer membranes and vesicles differ significantly depending on whether they are comprised of PC molecules or PE molecules. This is surprising in the light of the fact that the structures of PC and PE are not so very different. PC has three methyl groups at the N^+ end of the headgroup whereas PE has three hydrogens; moreover, as discussed earlier (2, 3), x-ray crystallography and neutron scattering experiments show that both types of headgroups have the same orientations, lying largely parallel to the plane of the bilayer under the experimental conditions. Nevertheless, their hydration characteristics and curvature effects, chain melting transitions, bilayer forces/fusagenic potential, charging and ion binding/transport control, and interactions with other membrane components are different and may contribute to their functionality and influence the composition of, and their localization within, specific membranes. Such observations lead to several questions, including: (*a*) What is the molecular basis for the different interactions among PC molecules on the one hand and PE molecules on the other? (*b*) How do the lateral interactions among phospholipid molecules contribute to the bilayer–bilayer interactions that occur when vesicles or biomembranes approach each other and fuse? In the papers here, we attempt to resolve the first question for dilute and semidilute layers as a prelude to establishing in later papers the interactions in more condensed layers and furnishing a model for the more difficult problem of bilayer–bilayer interactions.

The method of choice for obtaining information about lateral interactions among lipid molecules is the measurement of pressure-area isotherms in spread monolayer experiments. The surface density, Γ, is a known, controlled, independent variable and experiments can cover the range from the very dilute gaseous state up to close packing of the lipids. Being able to monitor interactions from very large average molecular separations down to the condensed state provides a powerful approach analogous to that used in the development of theories for three-dimensional systems. In the surface experiments we have the added advantage of insights into changes in dipole orientation from measurements of surface potential which compensates partially for the complexities raised by the subtleties of intra- and interlayer interactions of dipoles. The choice of a nonpolar

Address correspondence to Dr. Dill.

0006-3495/92/06/1603/13 $2.00

oil/water interface arises from the finding that the lateral pressure is not affected by the monolayer chains at surface densities below any surface phase transition. This was first deduced by Davies (4) from the behavior of semidilute monolayers of an equimolar mixture of oppositely charged lipids, later confirmed by the chain-length independence of the lateral pressure of long chain alkyl sulphates (5–7) and PC's (1, 10). As we will show below with C_{14} to C_{18}PC monolayers the chains also make no contribution to the surface potential over the same range of surface densities. This means that we can solely follow head group interactions. This is not the case for the air/water interface where both the pressure and the potential are affected by the monolayer chains interacting with the water surface where, at the same time, attractive interactions among the chains cause a variety of complicating surface phase transitions, some of them at extremely low surface densities. An added advantage of the oil/water interface is that the pressures in the dilute region are much higher than those at the air/water interface because of the lack of chain–chain cohesive interactions so that experimental errors are a smaller proportion of the measured pressure, and sensitive terms such as the virial coefficients can be extracted with much more confidence.

A large corpus of oil/water data obtained by one of us and his colleagues exists, much of it published piecemeal addressing mainly thermodynamic issues, typically by Taylor et al. (1), Yue et al. (8), and Pethica et al. (9). The bulk of the lateral pressure data at high surface densities encompassing a phase transition was published by Mingins et al. (10). In the present paper, we have brought together the remaining results for monolayers of very low surface densities and those already published, and extend their range to just below any phase transition. Furthermore, new data on surface potentials are added to those already published (9). In response to the very demanding requirements of the analysis of these dilute monolayers, we have checked the experimental results on all chain lengths much more critically for the spreading errors, monolayer leakage and spreading solvent retention discussed in a previous paper (12). By far the most common systematic error is that of monolayer loss on spreading. It manifests itself in poor reproducibility in isotherms of Π or ΔV from nominally the same volume of lipid solution spread and in a lack of overlap of Π (ΔV) isotherms obtained by compressing a series of spreads on top of existing stabilized monolayers. In the latter event, a scaling routine as described previously (10, 12) is adopted to obtain a full connected isotherm and this is done down to losses of 2%. Such routines taken together with the discard of runs showing either unstable Π (ΔV) or disjointed composite isotherms because of spreading solvent retention result in a much more rigorous set of isotherms which merge smoothly with those at higher surface densities presented by Mingins et al. (10).

Before developing our previous model further in part II we need to first establish in this paper the salient aspects of the behavior of PC and PE monolayers that have to be addressed with the theory. We shall first examine the surface potentials to check the effects of salt, pH, chain length (for PC only), and temperature and contrast the behavior of PC and PE. In particular, we are concerned to find out over what range of molecular separations the net average orientation of the phospholipid dipoles is uninfluenced by the lateral interactions among the phospholipid molecules. We include also for comparison some limited surface potential data on a PE containing both branched and olefin chains. With the lateral pressures we examine the same system variables as with the potential and again the data on saturated PE's are limited to only one chain length, namely tetradecyl. The data yield a more accurate set of experimental values of the second and third virial coefficients than hitherto. The following paper then presents a theoretical model that is consistent with these collective data which provide a stringent test for any theoretical approach.

Surface potentials

We used the vibrating plate electrometer method to measure the change in interfacial potential due to the phospholipid relative to a clean oil/water interface. This method was first applied to liquid surfaces by Yamins and Zisman (11), and in our studies is combined with the oil/water trough developed by Brooks and Pethica (6) to compress monolayers at the interface between *n*-heptane and an aqueous solution. The preparation of a clean interface and the procedures for obtaining an accurate lateral pressure-area isotherm for an insoluble monolayer at the interface of a nonpolar oil with water have been described by Taylor and Mingins (12) and also apply in the measurement of potentials. Because few studies of the surface potential have been described for compressed monolayers at the oil/water interface, and because most workers have relied on the uncertain method of continuous addition of surfactant to vary the surface density, we present here some of the salient features of the extra procedures needed to obtain accurate, reproducible surface potential-area isotherms.

The method of Yamins and Zisman (11) relies on measuring a so-called "compensation potential" by applying a DC potential P to null the small AC current flowing across the capacitor formed by the interface and a vibrating metal electrode. This is done in the presence and absence of the spread monolayer. The surface

potential of the monolayer, ΔV, is defined operationally as the difference between the two compensation potentials, $\Delta V = P(\text{monolayer}) - P(\text{water})$. The sensitivity of the method is proportional to the area of the vibrating electrode and the amplitude of the vibration and is inversely proportional to the separation of the electrode and the interface. In our experiments a thin rigid silver electrode (3×1 cm^2) is positioned in the oil accurately parallel to, and ~ 1 mm away from, a swept and aspirated interface in an oil-water trough. A suitable compromise between sensitivity and risk of aqueous wetting of the electrode during monolayer spreading and compression is obtained using this separation and an amplitude of vibration of ~ 0.05 mm. Of the many ways of establishing the compensation state, we chose to amplify the small AC current using a high-gain frequency-selective detector amplifier (tuneable to 1 hz) and compared the output on an oscilloscope with the stable signal driving the vibrating electrode. A schematic diagram of the apparatus is given in the paper by Pethica et al. (13). As the compensation state is approached, the driving and receiving signals are nearer in phase and at null current the Lissajous figure on the oscilloscope collapses to a horizontal line. With good shielding and the capacitor specifications given above, we achieved a discrimination better than 0.3 mV under optimal conditions.

Given stable electronics, the major factors governing the quality of the surface potential data are: lack of impurities, quantitative spreading, removal of the spreading solvent, and leakage-free compression. All these aspects were addressed in the measurement of lateral pressures (12). The compensation potential of the clean interface necessarily contributes to the measurement of the surface potential; it is this potential which is difficult to establish with confidence (14). The difficulty arises because compensation potentials are arbitrary, i.e., there is no fixed reference value. The only measurement of significance is the change, ΔV, brought about by spreading the monolayer. A valid P(water) should at least be constant with time and with compression or expansion of a clean surface. A routine which we have followed to insure a secure value of P(water) (and which, at the same time, validates the P[monolayer] values) arose from the observation that for a dilute phospholipid monolayer P(monolayer) was linear with the reciprocal of the separation (L) between the barriers defining the length of the working interface on the trough. Because the surface potential ΔV must vanish at infinite dilution of the monolayer, an extrapolation of P(monolayer) to $1/L$ equals zero should then give P(water) which, if all is well, should agree with the value obtained by the standard method of sweeping and sucking the surface instituted at the start of the run. Spreading additional lipid molecules on top of the initial monolayer should give overlap of the P(monolayer) when L is normalized for the new surface densities. A typical example of a satisfactory run is given in Fig. 1. If such agreement is not obtained, it is safest to discard the run, but the quality of the linear fit may justify rejecting the "sweeping" value. Both approaches have been adopted here to obtain the comprehensive set of potentials described below. For monolayer loss which may occur upon spreading we resort again to the scaling routine previously validated for the lateral pressure measurements (12). The final check on this type of scaling is that there must be congruence of the surface densities at which surface phase transitions are seen with both potentials and lateral pressures. Discussion of the phase transitions will be deferred to a subsequent paper.

The ΔV results on the PC monolayers which are shown in Figs. 2–4 indicate that: (*a*) the surface potential does not depend on concentration of NaCl, (*b*) the surface potential does not depend on alkyl chain length, and (*c*) there is a small but measurable increase in surface potential with temperature for PC.

Fig. 2 shows the surface potential, ΔV, versus the interfacial concentration, Γ, of typically diC_{14}PC at 20°C for two NaCl concentrations: 0.1 M and 0.01 M. Similar behavior (not shown) is obtained with other PC's and another salt concentration. In all cases the PC monolayer renders the heptane phase more positive than the water phase. It is well known that the addition of salt

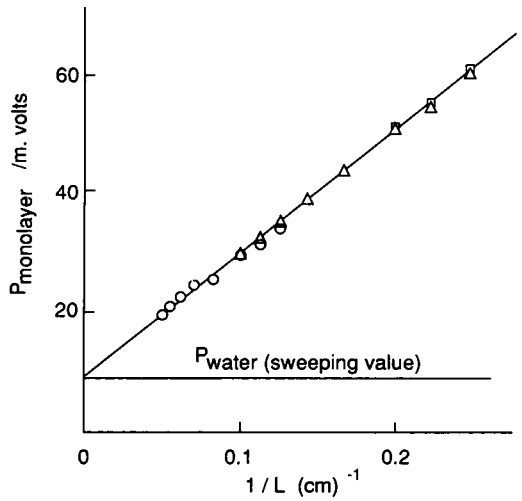

FIGURE 1 Compensation potential P(monolayer) versus the reciprocal of barrier separation ($1/L$) in compression studies on diC_{14}PE spread at the *n*-heptane/0.01 M NaCl interface at 20°C. Spreading volumes in ml: *circles*, 0.01; *triangles*, 0.02; *squares*, 0.04. The values of L are scaled to those of the run with 0.01 ml to compensate exactly for the increase in the number of molecules spread.

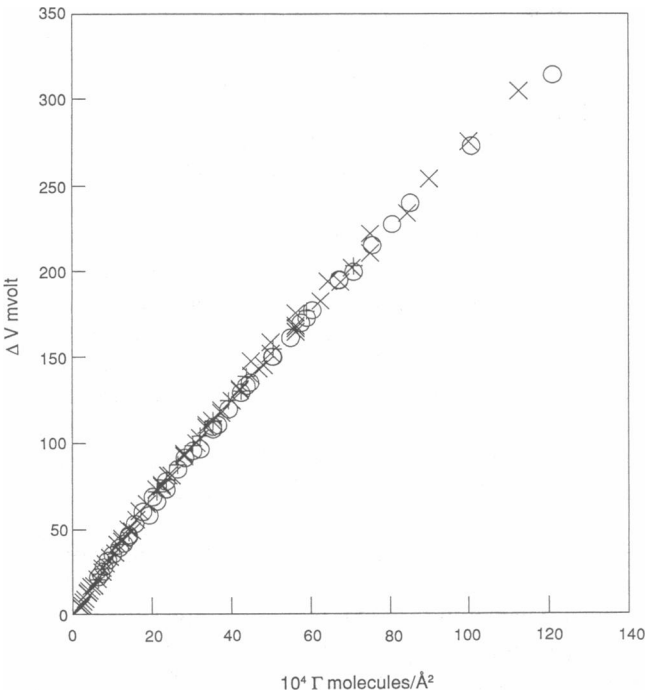

FIGURE 2 Surface potential, ΔV, versus Γ for $diC_{14}PC$ at 20°C at the interface between *n*-heptane and aqueous solutions: salt and pH-dependence. +: 0.1 M NaCl; X: 0.01 M NaCl; O: 0.01 M HCl.

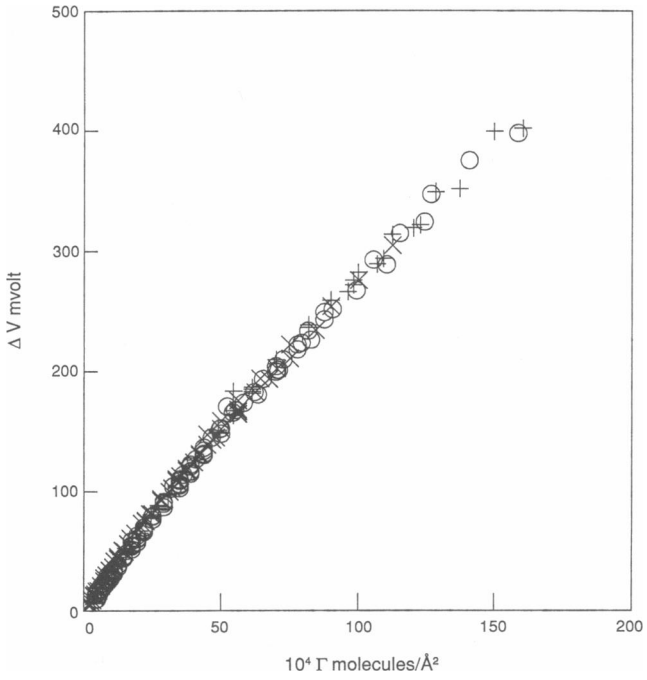

FIGURE 3 Surface potential, ΔV, versus Γ at 20°C at *n*-heptane/0.01 M NaCl interface for diRPC for various chain lengths. X: R = C_{14}; +: $R = C_{16}$; O: $R = C_{18}$.

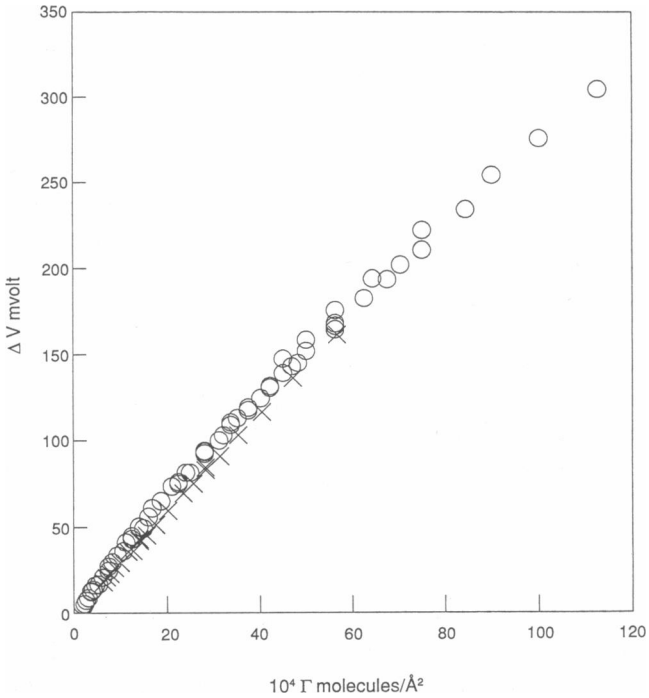

FIGURE 4 Surface potential, ΔV, versus Γ for $diC_{14}PC$ at *n*-heptane/0.01 M NaCl interface as a function of temperature. X: 10°C; O: 20°C.

shields (Coulombic) interaction between single charges (but not between point dipoles) giving a salt dependence of ΔV for charged monolayers depending on the primary charge density of the monolayer (15). Under the conditions of these experiments, at pH = 5.5, the PC headgroup has no net charge. This is confirmed by the lack of a salt effect in the ΔV data. Also, as seen in Fig. 2, reducing the pH to 2.1 has no effect on ΔV for $diC_{14}PC$, in keeping with the behavior of the lateral pressure for both $diC_{14}PC$ (10) and $diC_{18}PC$ (8) and as expected from the electroneutrality of the PC head group in this pH range.

A comparison of ΔV for $diC_{14}PC$, $diC_{16}PC$ and $diC_{18}PC$ at 20°C in Fig. 3 shows no chain length dependence at Γ below any phase transition, evidence that the hydrocarbon chains of these lipids do not contribute significantly to ΔV. The few surface potentials available on $diC_{22}PC$ (not shown) are marginally lower than those of the other PC's. This may indicate a slight effect of the eight extra methylene groups on dipole orientation which would be difficult to explain, particularly in view of the agreement in Π for all the PC's over the same range of surface density. At this stage we just draw attention to the anomaly and defer publication of these limited ΔV data on $C_{22}PC$ until the situation is resolved one way or the other with further experiments. We would expect the interfacial water dipoles not to distinguish between the

methylene groups of the phospholipids and those of the heptane phase unlike at the air/water interface where lipid chain reorientation of the interfacial water dipoles is possible.

A small but significant increase in ΔV with increase of temperature is shown for $diC_{14}PC$ in Fig. 4. The range of surface densities over which comparisons can be made is rather small because of the paucity of reliable data at 10°C. However, an increase of ΔV with temperature for PC's was unambiguously shown in the data of Sehgal et al. (16) on $DiC_{18}PC$ at the 2,2,4-trimethylpentane/water interface. Using the much greater temperature span of 25.5°C they obtained the substantial increase of ~30 mV for example at a surface density of 1 molecule/nm^2. No great emphasis should be placed on their results at low surface densities though because they do not go through the origin.

Next, we consider the surface potentials for PE molecules. Surface potentials of $diC_{14}PE$ at the heptane/aqueous electrolyte interface which were first reported by Pethica et al. (9) are shown in Fig. 5 with additional results. Again, the monolayer makes the heptane phase more positive with respect to water. As with the PC monolayers, there is no dependence of ΔV on the NaCl concentration. Unlike the PC data of Fig. 4, there is no increase of ΔV with temperature. For our purposes we regard the potentials as constant within the scatter shown although a slight decrease in ΔV with increase of temperature may be operating. If this is indeed the case it merely strengthens our arguments below. Fig. 5 shows that the surface potentials for PE are dependent on pH. Upon addition of 0.1 M HCl, ΔV for $diC_{14}PE$ is significantly more positive than it is at neutral pH in NaCl solutions. Similar behavior was found by Standish and Pethica (17) for the surface potential of $diC_{16}PE$ monolayers at the air/water interface. Their calculated value of 0.32 for the surface pK_a of the phosphate group is considerably lower than the first pK_a of phosphoric acid (2.12) or amino-ethyl phosphoric acid (2.45) in bulk solution. Our model of the PE head group is in agreement with this incomplete ionization of the phosphate group of the PE where at neutral pH the N^+ charge is compensated by the P^- charge at the interface, but at low pH by a mobile Cl^- ion that on average is away from the interface, further into the aqueous solution. This change of distribution of negative charge at low pH from the interface into the water makes the potential relatively more positive in the hydrocarbon phase. There is no reason to expect a dependence on pH of the (average) position of the N^+ charge in the present experiments. The results on $diC_{14}PC$ in Fig. 2 show no net charge on 0.01 M HCl.

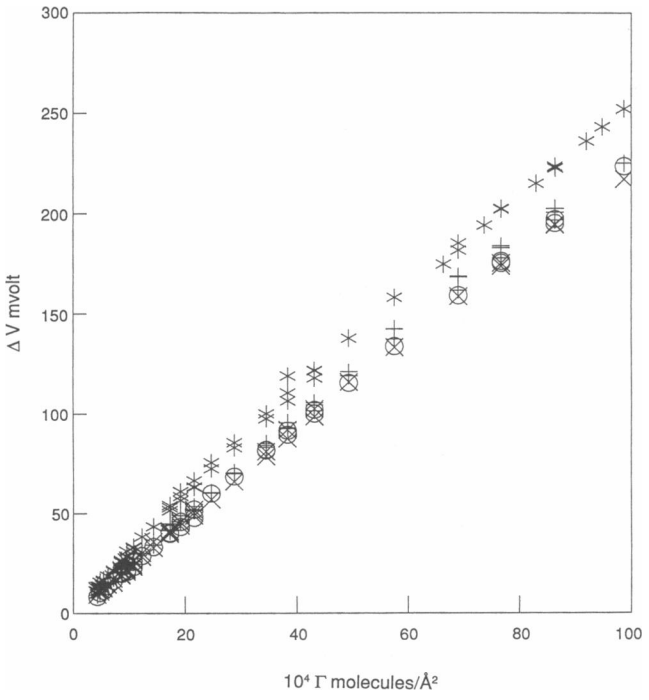

FIGURE 5 Surface potential, ΔV, versus Γ for $diC_{14}PE$ at the interface between *n*-heptane and aqueous solutions: salt and pH-dependence. O: 0.1 M NaCl at 20°C; X: 0.01 M NaCl at 20°C; +: 0.01 M NaCl at 6°C; *: 0.1 M HCl at 20°C.

Next, we consider PE molecules with a different type of alkyl chain. Fig. 6 shows ΔV versus Γ for various monolayers of oleoyl-isolauroyl PE. For NaCl solutions the data do not differ significantly from those for $diC_{14}PE$ in Fig. 5. This suggests that head group and water dipoles dominate in ΔV, and that the olefinic bond does not contribute to or affect the water orientations at the monolayer surface. This contrasts with expanded monolayers of oleic acid at the air/water interface (18). Using air/water data various authors have argued that the terminal methyl group of lipid chains makes a significant contribution to ΔV. For example, Vogel and Möbius (19) estimate a dipole moment of 0.35 D directed from monolayer to air. The superposition of ΔV for $diC_{14}PE$ and those for oleoyl-isolaurylPE means that the extra methyl group of the latter does not contribute to ΔV at the heptane/water interface over the range of surface densities shown and by implication that the other methyl groups do not contribute either. The difference between the NaCl and 0.01 M HCl data for the oleoyl-isolauroyl PE (Fig. 6) is smaller than that between the NaCl and 0.1 M HCl data for the *n*-alkyl PE (Fig. 5), as expected from models with a pH dependent phosphate charge at the interface because the monolayers on 0.1 M have a greater net charge than on 0.01 M HCl.

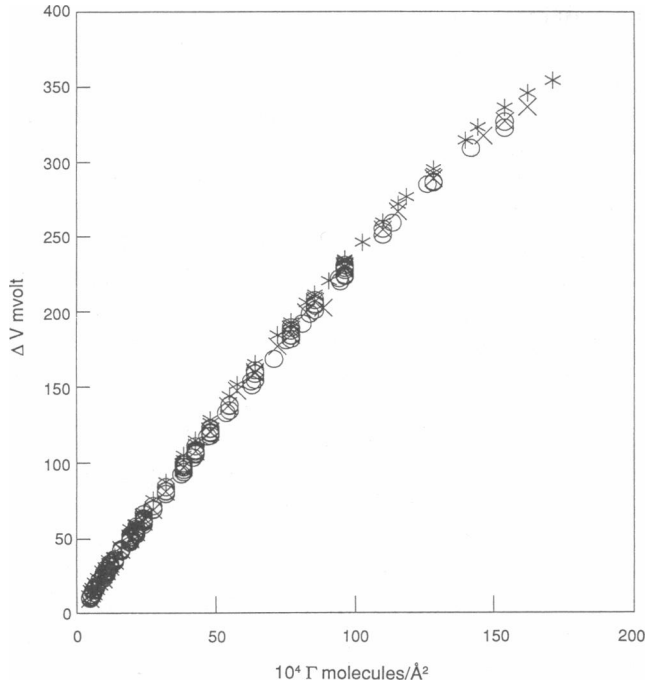

FIGURE 6 Surface potential, ΔV, versus Γ of oleoyl-isolauroylPE at the interface between *n*-heptane and aqueous solutions at 20°C: salt and pH-dependence. X: 0.1 M NaCl; O: 0.01 M NaCl; *: 0.01 M HCl.

Our measured ΔV is a difference in compensation potentials and as such can be taken as $\Delta\chi$, the change in true surface potential (χ) brought about by spreading a monolayer (20). The potential χ is the potential drop across the interfacial dipoles in the compensated state. Although it has been criticized on several counts (see for instance, reference 14) the Helmholtz relation in classical units,

$$\Delta V = 4\pi\Gamma\mu_s, \tag{1}$$

applied by Schulman and Rideal (21) to fatty acid monolayers forms a useful starting point for a discussion of ΔV. Here Γ is again the surface number density of monolayer molecules and μ_s is the net surface dipole moment of the monolayer molecule. Water molecules at a clean interface orient under the action of neighboring water dipoles, thereby setting up the χ-potential and forming a molecular layer difficult to characterize with its unknown extent and density. The χ-potential itself is not measurable. The addition of a spread monolayer introduces to this milieu a new set of dipoles of unknown location and orientation which are governed by their interactions with the phases making up the interface as well as by the interactions among themselves. A new χ-potential results which is again not measurable. Values of μ_s calculated from ΔV data using Eq. 1 are always substantially lower than the intrinsic dipole moments of the monolayer molecules. This has been rationalized in terms of the macroscopic quantity, ΔV, measuring the average net components of the oriented monolayer dipoles in a solvent normal to the interface (22, 23) plus the change in the normal components of the solvent dipoles. A dielectric constant of unity was taken to apply in Eq. 1 with solvent effects subsumed in the μ_s term. Calculation of μ_s from ΔV via Eq. 1 thus gives an average effective value for a composite term, and some authors have preferred to limit discussion to such a net moment (see for example, reference 14), which would be better designated $\Delta\mu_s$ to emphasize that it covers a change in the surface dipole term.

Because ab initio calculation of potentials from the individual bond moments in the monolayer and solvent(s) molecules is not feasible, polarization effects are usually approximated by introducing a dielectric constant. Typically Eq. 1 would now read

$$\Delta V = 4\pi\Gamma\frac{\Delta\mu_s}{\epsilon_e}, \tag{2}$$

where ϵ_e is an effective dielectric constant of the monolayer region. However, if dipoles reside in both the nonaqueous and aqueous phases then, as Pickard et al. (24) point out "no choice of ϵ_e will yield a strictly meaningful $\Delta\mu_s$." Demchak and Fort (25) have taken Eq. 2 further by splitting $\Delta\mu_s$ into dipole contributions from water dipoles (μ_1), monolayer dipoles in the water (μ_2) and monolayer dipoles out of the water (μ_3) and scaling each with an effective dielectric constant for the medium in which each dipole resides (D_1, D_2 and D_3, respectively). The terms D_2 and D_3 include everything which causes the moments of the monolayer groups to deviate from the values they would have in the isolated molecules in bulk solvent whereas in μ_1/D_1 is incorporated the polarization of the water by the monolayer.

In developing a theory of phospholipid interactions at the heptane/water interface we choose to take D_2 and D_3 as ϵ_w and ϵ_h, the respective bulk dielectric constants of water and heptane and like Demchak and Fort (25) gather any changes to the water into a term corresponding to their μ_1/D_1. With each bulk phase treated as a continuum up to the planar interface we can use the method of electrostatic images to handle average field quantities, interactions, et cetera in Part II. To check the form of the contribution to ΔV consider then two

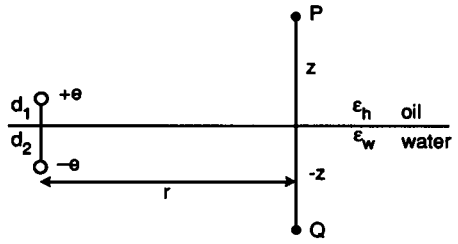

FIGURE 7 Charge disposition near dielectric boundary with dipole potential across interface in Eq. 1.

dipoles, ed_1 in heptane and ed_2 in water, next to each other at the heptane/water interface (see Fig. 7). With the help of image charges, we can find the potential across the interface, at distance r from the dipoles. Dispensing with classical units, this reads,

$$\Delta V = \Psi_P - \Psi_Q = \frac{2z}{4\pi\epsilon_0(r^2 + z^2)^{3/2}}\left(\frac{ed_1}{\epsilon_h} + \frac{ed_2}{\epsilon_w}\right) \quad \text{for } z \gg d_1, d_2, \quad (3)$$

where $e = 1.60 \times 10^{-19}$ Coulomb is the proton charge, and $\epsilon_0 = 8.85 \times 10^{-12}$ Farad/m is the permitivity of vacuum.

To show that Eq. 3 leads to classical results, we first consider two uniformly charged surfaces, one at the interface ($d_2 = 0$), the other at distance d_1 into the heptane, with surface charge density $-\Gamma e$ and Γe, respectively. For this case, Eq. 3 leads, after integration over the surface charge, to the well known expression for the flat plate capacitor,

$$\Delta\Psi = \frac{\Gamma}{\epsilon_0}\frac{ed_1}{\epsilon_h}. \quad (4)$$

If instead the lower plate of this capacitor is moved a distance d_2 from the interface into the water, Eq. 3 yields

$$\Delta\Psi = \frac{\Gamma}{\epsilon_0}\left(\frac{ed_1}{\epsilon_h} + \frac{ed_2}{\epsilon_w}\right). \quad (5)$$

Adding the change in water dipoles to this would give ΔV for this set of dipoles.

There are three significant dipolar contributions that might arise from the introduction of phospholipids to the oil/water interface. First μ_{PN}, the P^-N^+ vector of the zwitterionic head group of length $\sim 1 = 4.5$ Å which may point into either bulk phase, gives a maximum out-of-plane dipole moment of $le = 4.5 \times 4.8 = 22$ debye (1 debye $= 3.33 \times 10^{-30}$ Coulomb meter). (Because our ΔV is taken as positive when the heptane becomes more positive with respect to water on spreading a monolayer, the P^-N^+ vector pointing toward the water would make a negative contribution to ΔV). Second, μ_{GL}, from the ester linkages, each of which has a dipole moment of 1.8 debye between the glycerol backbone of the phospholipid and the hydrocarbon chains, might contribute at most 1 debye per lipid molecule to the total out-of-plane dipole moment in heptane (2). Finally, there is the change in the average orientation of water molecules in the neighborhood of the phospholipid ($\Delta\mu_w$); each water molecule has a dipole moment of 1.84 debye. This contribution might be substantial but is difficult to quantify. In summary, there may be positive and negative contributions to ΔV and it is likely they are all significant. Couching these dipole terms in the appropriate format for Eq. 3 gives

$$\Delta V = \frac{\Gamma}{\epsilon_0}\Sigma\frac{\mu}{\epsilon}, \quad (6)$$

where

$$\Sigma\frac{\mu}{\epsilon} = \frac{\mu_{PN}}{\epsilon_x} + \frac{\mu_{GL}}{\epsilon_h} + \frac{\Delta\mu_w}{\epsilon_w}, \quad (7)$$

with $\epsilon_x = \epsilon_h$ or ϵ_w depending on whether the P^-N^+ vector is in the heptane or the water. Eq. 6 is similar to that used in the papers by Sehgal et al. (16) and Pickard et al. (24), save for the one respect that we allow the positive pole of the phospholipid zwitterion to swing into the heptane, the negative phosphate charge remaining at the interface. As will be seen in Part II, this is crucial in explaining the PC data on lateral pressures.

Returning now to the ΔV data we note that the ΔV–Γ plots can be taken as linear in the low Γ range. The expanded plots in Fig. 8 for typical $diC_{14}PC$ and $diC_{14}PE$ data illustrate the point more clearly. This is evidence that each molecule contributes independently to the net dipole moment at these low concentrations. In other words, the lateral interactions between two or more phospholipid molecules here are not causing the orientation of individual dipoles to depend on lipid concentration. Thus, the limiting slope of the curves is proportional to the dipole contribution per lipid molecule. To give some idea of size, if we scale the slopes with the proton charge to give dimensions of length we find from Eq. 6 that $\Sigma(\mu/e\epsilon) = 0.130$ Å for PE at 6° and 20°C, 0.164 Å for PC at 10°C and 0.189 Å for PC at 20°C. Although these figures in themselves are by no means a definitive list of head group orientations, nevertheless we suggest that the difference in surface potential say for PC at one temperature compared to PC at another, or for PE at two different temperatures, or for PE and PC

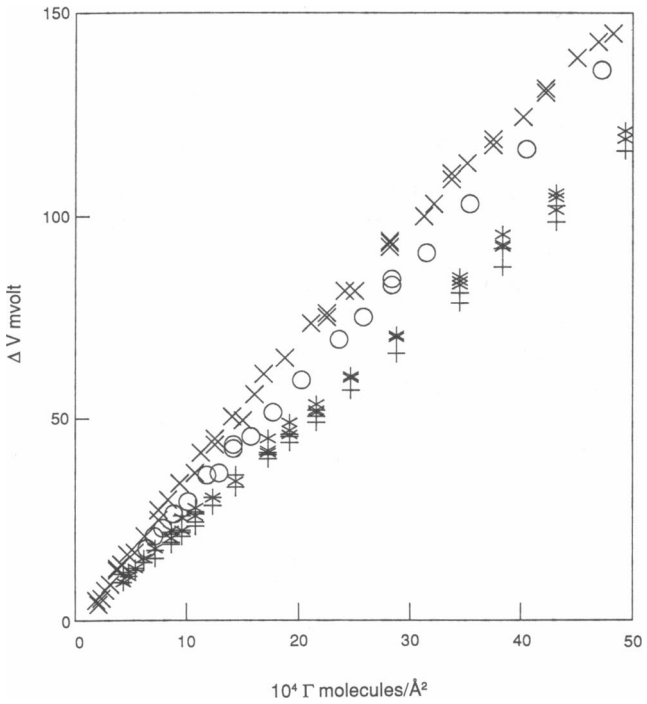

FIGURE 8 Surface potential, ΔV, versus Γ for $diC_{14}PE$ and $diC_{14}PC$ at the *n*-heptane/0.01 M NaCl interface: head group and temperature-dependence. O: $diC_{14}PC$ at 10°C; X: $diC_{14}PC$ at 20°C; *: $diC_{14}PE$ at 6°C; +: $diC_{14}PE$ at 20°C.

at the same temperature, will be useful for comparing models of head group orientation.

For PE the limiting slope of the ΔV curves does not depend on temperature, see Figs. 5 and 8. Therefore, it is reasonable to assume that none of the three contributions to ΔV in Eq. 7 is temperature dependent for PE and, further, that this constancy holds also for the contributions of ester and water dipoles to ΔV in the case of a PC monolayer. It then follows that the difference with temperature between the two PC curves in Fig. 8 must be caused by the P^-N^+ orientation of the PC head group. This is consistent with the theoretical model (2) for PC, which predicts that the N^+ becomes more immersed in heptane with increasing temperature. The data above show that the difference between 10° and 20°C in $\Sigma(\mu/e\epsilon)$ is 0.189 − 0.164 = 0.025 Å for PC and this is limited to changes in $\mu_{PN}/e\epsilon_x$. Because ΔV becomes more positive at the higher temperature, the P^-N^+ vector must point more toward the heptane. If this vector is always in the heptane then with $\epsilon_x = \epsilon_h \approx 2$, the difference between the slopes at 10° and 20°C would correspond to an average rise of N^+ in the heptane of about 0.05 Å. The finding that ΔV for PE does not increase with temperature would indicate that there is no such swing of the more exposed N^+ charge of the ethanolamine group in PE over the temperature range studied.

The above comparison of the slopes of the PC and PE curves at the same temperature shows that $\Sigma(\mu/e\epsilon)$ is much more positive for PC. The ester dipoles are identical in the two molecules so that the μ_{GL}/ϵ_h term should contribute similarly to ΔV. Moreover, a large proportion of the zwitterion is also identical in PC and PE and it would be reasonable to expect that any difference in $\Delta\mu_w$ would give a secondary term, particularly when it is reduced by scaling with ϵ_w. Consequently, the difference in ΔV between PC and PE monolayers would again be largely attributable to μ_{PN} with the P^-N^+ vector pointing more toward the heptane for PC, in keeping with the temperature data.

The ΔV plots over the full range depicted show a slight curvature, see Figs. 2 to 6. This could, in principle, arise from lateral interactions among lipid chains or head groups. We dismiss the former at this interface because of the chain length-independence of both ΔV and lateral pressure at surface densities below those of any phase transition. If the mutual interaction between P^-N^+ dipoles would cause their average orientation to change with coverage, then this would cause a curvature of the ΔV–Γ plot and, at the same time, contribute to the third virial coefficient of the lateral pressure (3). In that case one would expect the ΔV–Γ curvature for PE with P^-N^+ dipoles in water to be several orders of magnitude smaller than for PC with P^-N^+ dipoles in heptane. However, the PE graphs in Figs. 5 and 6 show similar curvature as the PC graphs in Figs. 2 to 4. A more likely explanation of this small and rather uncertain curvature is a change of average orientation of water molecules between approaching head groups. We feel justified in assuming that the average tilt of the P^-N^+ dipoles is constant over the concentration range we address with the virial approach.

Pressure-area isotherms and the virial coefficients

In addition to surface potentials, we present data here on pressure-area isotherms for the PC and PE monolayers. We use the two-dimensional virial expansion to describe deviations from ideal behavior. The nonideality is captured in the second and third virial coefficients which provide information on the lateral headgroup interactions. For monolayers that obey the two-dimensional ideal gas law, the lateral pressure Π and the interfacial concentration Γ are related by $\Pi = kT\Gamma$ where k is Boltzmann's constant and T is the absolute

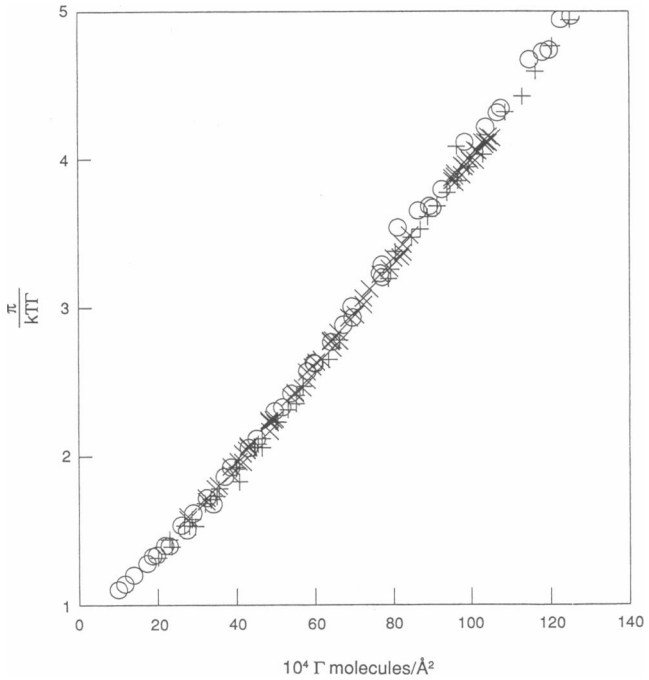

FIGURE 9 $\Pi/kT\Gamma$ $(=1 + B_2\Gamma + B_3\Gamma^2 + \ldots)$ versus Γ for diRPC at the *n*-heptane/0.01 M NaCl interface at 10°C-chain length-dependence. +: $R = C_{14}$; O: $R = C_{16}$; X: $R = C_{18}$.

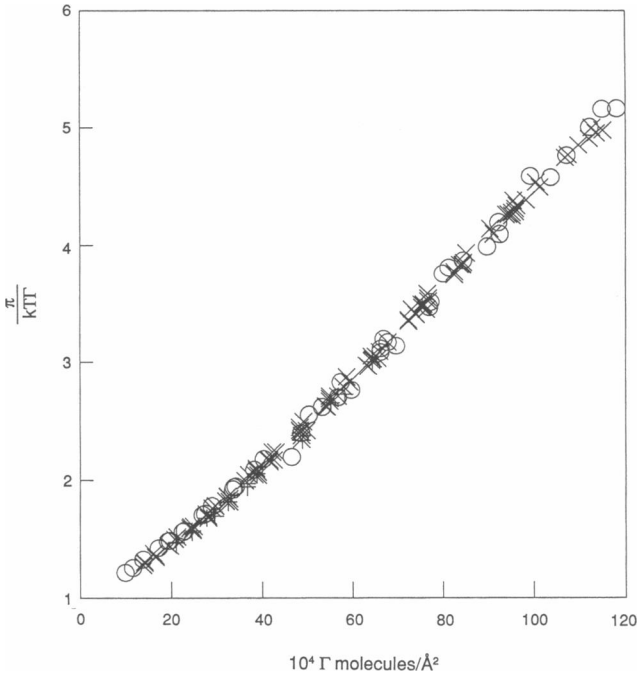

FIGURE 10 $\Pi/kT\Gamma$ $(=1 + B_2\Gamma + B_3\Gamma^2 + \ldots)$ versus Γ for diRPC at the *n*-heptane/0.01 M NaCl interface at 20°C-chain length-dependence. O: $R = C_{16}$; X: $R = C_{18}$; +: $R = C_{22}$.

temperature. In Figs. 9 and 10 $\Pi/kT\Gamma$ is plotted versus Γ at 10 and 20°C for monolayers of PC lipids of various chain lengths, spread between aqueous 0.01 M NaCl solutions and *n*-heptane. As seen hitherto (1) the data show large deviations from the ideal value, $\Pi/kT\Gamma = 1$, which are independent of chain length in the C_{14} to C_{22} range. This shows that the lipid hydrocarbon chains do not contribute to the nonideality of Π, which therefore depends only on the lateral headgroup interactions.

Figs. 11 and 12 show $\Pi/kT\Gamma$ versus Γ for monolayers of $diC_{18}PC$ and $diC_{22}PC$ at 20°C in contact with 0.1, 0.01, and 0.001 M NaCl. There is no dependence of Π on salt concentration, in keeping with the earlier published isotherms (1, 8) and consistent with the ΔV data on $diC_{14}PC$ in Fig. 2. We attribute the nonideality of II principally to steric and dipolar repulsions from the large finite dipole due to the P^-N^+ separation.

The most extensive data are available for $diC_{18}PC$ in 0.01 M NaCl at 5° to 25°C, shown in Figs. 13 and 14 as plots of $\Pi/kT\Gamma^2 - 1/\Gamma$ versus Γ. At each temperature the data are well represented by a four term polynomial

$$\frac{\Pi}{kT} = \Gamma + B_2\Gamma^2 + B_3\Gamma^3 + B_4\Gamma^4. \quad (8)$$

Linear regression analysis yields the virial coefficients B_i in Table 1. The values in parenthesis are the earlier results for B_2 and B_3 (3) that were obtained from Π data in a much narrower concentration range, up to $\Gamma = 5 \times 10^{-3}$ instead of $\Gamma = 12 \times 10^{-3}$, see Figs. 13 and 14. The present results are, therefore, more reliable. B_2 is somewhat lower than before, B_3 is higher and does not show the earlier temperature dependence. The negative, approximately constant values of B_4 are new results.

The scatter of points in Figs. 13 and 14 corresponds at each temperature to the experimental scatter in Π of ~ 0.05 dyne/cm, as in the earlier work (3). This error in Π, however, cannot be related directly to the uncertainty of the coefficients B_i of the fitted Eq. 8 because Eq. 8 is not

TABLE 1 **Two dimensional pressure virial coefficients in $diC_{18}PC$ monolayers at 0.01 M NaCl-heptane interfaces**

T°C	B_2Å²*	$B_3 \times 10^{-3}$*Å⁴	$B_4 \times 10^{-5}$Å⁶
5	115.3 ± 3.4 (125)	29.3 ± 0.1 (21.7)	−12.8 ± 0.4
10	133.5 ± 1.0 (156)	31.4 ± 0.2 (20.1)	−14.8 ± 0.1
15	155.0 ± 5.9 (187)	31.5 ± 2.4 (17.8)	−14.2 ± 2.0
20	177.6 ± 5.7 (218)	30.2 ± 1.1 (15.4)	−13.2 ± 0.4
25	226.6 ± 6.1 (249)	31.2 ± 1.7 (14.7)	−14.1 ± 1.2

*Values in parenthesis obtained earlier from more restricted data (3).

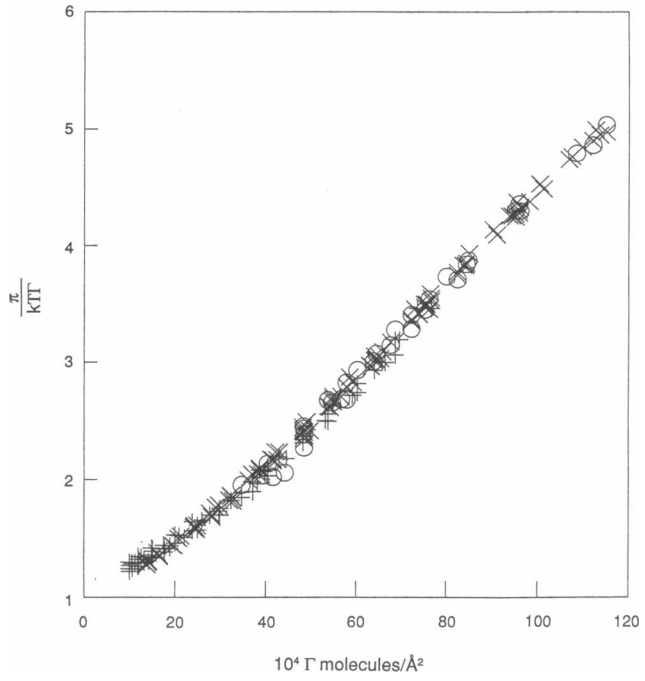

FIGURE 11 $\Pi/kT\Gamma\ (= 1 + B_2\Gamma + B_3\Gamma^2 + \ldots)$ versus Γ for $diC_{18}PC$ at 20°C at the interface between *n*-heptane and various aqueous NaCl solutions. O: M_{NaCl} = 0.1 M; X: M_{NaCl} = 0.01 M; +: M_{NaCl} = 0.001 M.

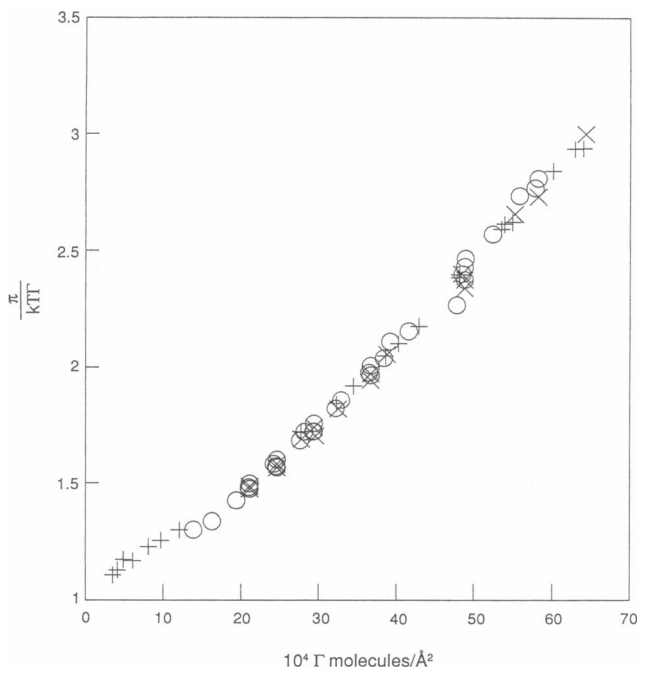

FIGURE 12 $\Pi/kT\Gamma\ (= 1 + B_2\Gamma + B_3\Gamma^2 + \ldots)$ versus Γ for $diC_{22}PC$ at 20°C at the interface between *n*-heptane and various aqueous NaCl solutions. O: M_{NaCl} = 0.1 M; X: M_{NaCl} = 0.01 M; +: M_{NaCl} = 0.001 M.

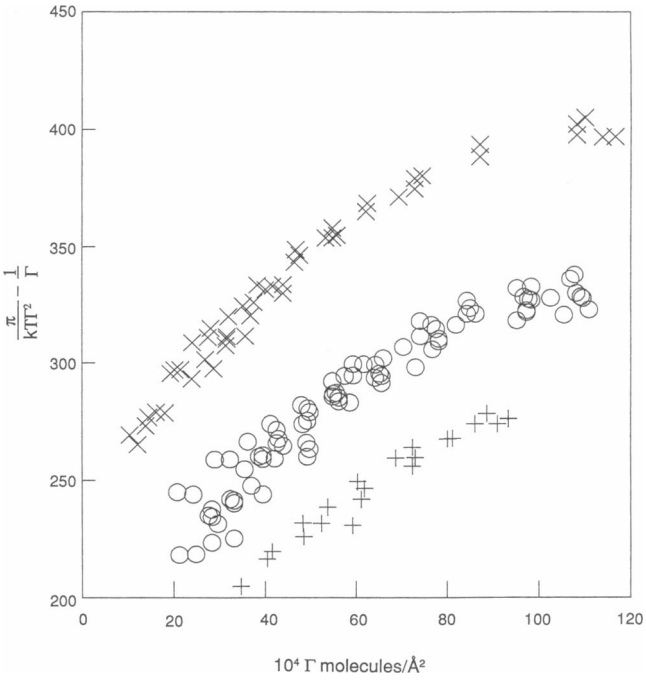

FIGURE 13 $\Pi/kT\Gamma^2 - 1/\Gamma\ (= B_2 + B_3\Gamma + \ldots)$ versus Γ for $diC_{18}PC$ at the *n*-heptane/0.01 M NaCl interface as a function of temperature. +: 5°C; O: 15°C; X: 25°C.

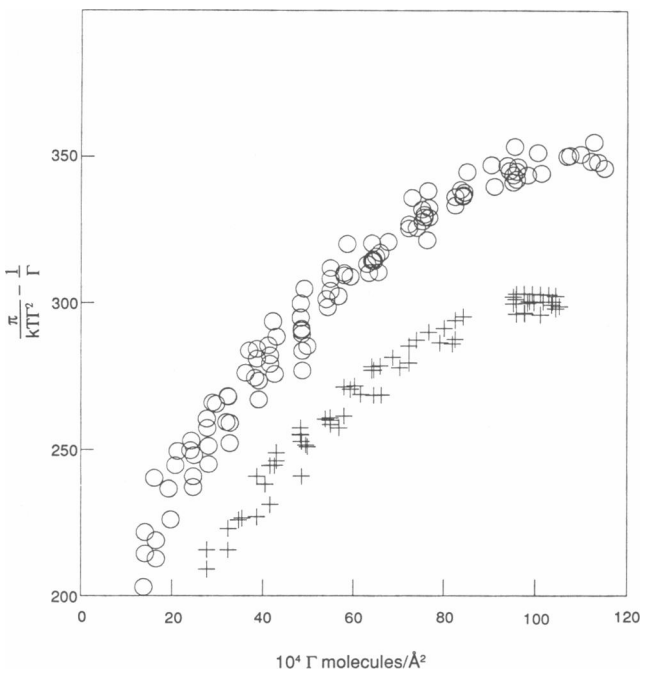

FIGURE 14 $\Pi/kT\Gamma^2 - 1/\Gamma\ (= B_2 + B_3\Gamma + \ldots)$ versus Γ for $diC_{18}PC$ at the *n*-heptane/0.01 M NaCl interface as a function of temperature. +: 10°C; O: 20°C.

an orthogonal polynomial. This can be seen graphically in Figs. 13 and 14 where B_2 is the intercept and B_3 is the limiting slope of the best line through a set of points. In fitting the data the effect of a too high intercept (B_2) can be partly compensated by a too low limiting slope (B_3). Hence, the errors in the B_i's from Eq. 8 are correlated with each other and were estimated as explained below.

Fig. 15 shows the B_2 values for $diC_{18}PC$ in 0.01 M NaCl from Table 1 as filled circles. Also shown are the B_2 results derived from the other runs for $diC_{14}PC$ to $diC_{22}PC$ on 0.1 M, 0.01 M and 0.001 M NaCl solutions where available. All results follow the same marked trend with temperature, but there is considerable scatter. The errors of B_2 depend on the range of Γ of available Π data and also on the total number of data points. For example, for $diC_{22}PC$ the two-dimensional gas/liquid phase transition limited the range of Γ to little more than half of that for the shorter chains. This explains the large scatter of the B_2 results of C_{22} in Fig. 15. Furthermore, the large variation of B_2 results at 20°C correlates well with the number of data points in each case which was, from low to high B_2, 32, 108, 21, 153, 17, 30, and 45. The results from the two longest runs cluster near the center and are obviously more accurate than the outlying values in Fig. 15. For these reasons the B_2 values from the extensive runs for $diC_{18}PC$ on 0.01 M NaCl are taken as representative and used for analysis in the following paper.

TABLE 2 **Two dimensional pressure virial coefficients in PE monolayers at aqueous NaCl-heptane interfaces**

T°C	M_{NaCl}	B_2Å^2	$B_3 \times 10^{-3}$Å^4	$B_4 \times 10^{-5}$Å^6
5	0.01	127.6 ± 16.2	20.0 ± 4.0	−7.8 ± 2.6
20	0.01	111.0 ± 5.8	22.2 ± 2.0	−8.0 ± 1.4
20	0.1	123.6 ± 25.6	20.0 ± 7.0	−6.6 ± 4.1

The accuracy of the B_i values from Eq. 8 increases presumably as the square root of the number of (Π, Γ) data points. Therefore, the error estimates ΔB_i in Tables 1 and 2 were obtained as follows. For each entry in the Tables the (Π, Γ) data were sorted into two equivalent sets by grouping odd and even entries in the data list. Eq. 8 was then applied to each of the two sets, producing two groups of B_i values whose differences divided by $\sqrt{2}$ are given as the uncertainties of the B_i's in Tables 1 and 2. The B_i values in Tables 1 and 2, obtained with Eq. 8 from the full sets of data, differ from the relevant averages of the two groups discussed above. This may show that the error analysis does not follow simple rules and, hence, Tables 1 and 2 give only a crude estimate of the errors.

The experimental data on PE are more limited than on the PC lipids. Fig. 16 shows $\Pi/kT\Gamma$ versus Γ for $diC_{14}PE$ monolayers under various conditions. The re-

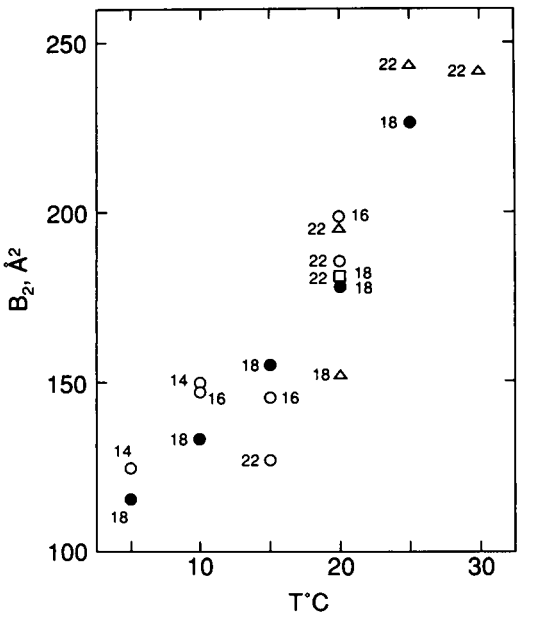

FIGURE 15 Second virial coefficient B_2 versus temperature for monolayers of diRPC at interface between *n*-heptane and aqueous NaCl solutions. R = 14 to 22 as shown by numbers in figure. *Triangles:* 0.1M NaCl. *Open and filled circles:* 0.01M NaCl. *Squares:* 0.001M NaCl.

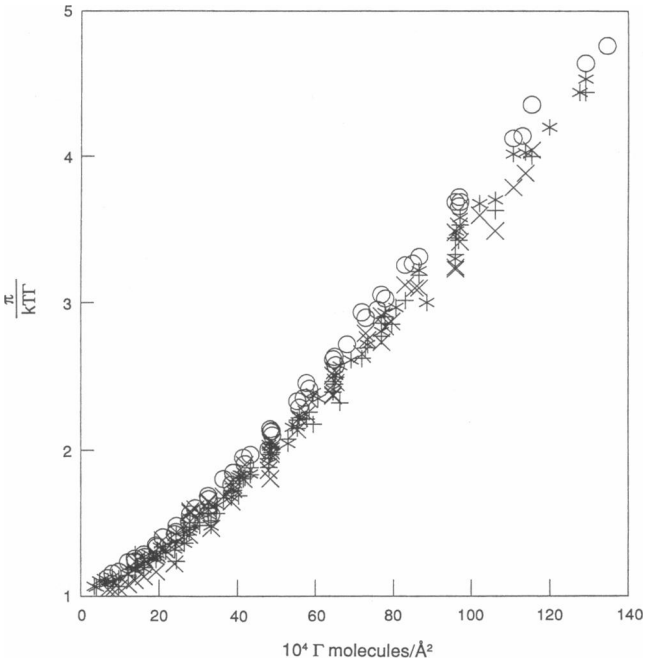

FIGURE 16 $\Pi/kT\Gamma$ ($= 1 + B_2\Gamma + B_3\Gamma^2 + \ldots$) versus Γ for $diC_{14}PE$ at the interface between *n*-heptane and aqueous solutions: salt and pH-dependence. X: 0.01 M NaCl at 5°C; +: 0.01 M NaCl at 20°C; *: 0.1 M NaCl at 20°C; O: 0.1 M HCl at 20°C.

sults on 0.01 M NaCl at 20°C were shown in a different plot in (9). Table 2 presents B_2, B_3, and B_4 for the monolayers against neutral NaCl solutions. These results show no significant dependence on NaCl concentration or on temperature, as is evident also by inspection of Fig. 16. For 0.1 M HCl, however, the pressures in Fig. 16 are slightly higher than for NaCl. This is evidence for charging of the monolayer due to the incomplete ionization of the PE phosphate group in 0.1 M HCl, consistent with the effect of HCl on ΔV in Fig. 5.

Conclusions

We have presented measurements of interfacial potentials and pressure-area isotherms of monolayers of PC and PE at the interface between n-heptane and water. For low to intermediate surface densities, we find that the surface potentials and lateral pressures are independent of chain length and NaCl concentration; they are therefore consequences of the headgroups. The surface potentials are net positive in the heptane phase. When PE becomes ionized at low pH, the surface potential becomes more positive due to a shift of negative charge from the interface (on the phosphate group at neutral pH) to the water phase (on the mobile Cl^- in the aqueous phase). At low surface densities, the interfacial potential is linear in surface concentration, indicating that each headgroup dipole acts independently at those concentrations. For PC, increasing the temperature leads to a more positive potential in the heptane phase, consistent with theory (2) predicting that the N^+ end of the headgroup dipole moves further into the oil phase with temperature, essentially independent of coverage. In the following paper, the virial coefficients and the associated temperature dependences determined here are used to test theoretical model predictions.

This and the following paper have evolved out of a series of papers involving one of us (J. Mingins) and papers by D. Stigter and K. A. Dill (many referenced herein). It is a pleasure then for J. Mingins to thank J. A. Gordon Taylor, Brian A. Pethica, Craig M Jackson, Eduardo Llerenas, and George M. Bell for the fun and excitement of jointly progressing this area.

We thank both North Atlantic Treaty Organization (NATO) and National Institutes of Health for financial support.

Received for publication 15 April 1991 and in final form 7 January 1992.

REFERENCES

1. Taylor, J. A. G., J. Mingins, and B. A. Pethica. 1976. Phospholipid monolayers at the *n*-heptane/water interface. Part 2. Dilute monolayers of saturated 1,2-diacyl lecithins and cephalins. *J. Chem. Soc. Faraday Trans. I* 72:2694–2702.
2. Dill, K. A., and D. Stigter. 1988. Lateral interactions among phosphatidylcholine and phosphatidylethanolamine head groups in phospholipid monolayers and bilayers. *Biochemistry* 27:3446–3453.
3. Stigter, D., and K. A. Dill. 1988. Lateral interactions among phospholipid head groups at the heptane/water interface. *Langmuir.* 4:200–209.
4. Davies, J. T. 1952. The application of the Gibbs equation to charged monolayers and their desorption from the oil-water interface. *Trans. Faraday Soc.* 48:1052–1061.
5. Phillips, J. N., and E. K. Rideal. 1955. The influence of electrolytes on gaseous monolayers. II. Ionized films. *Proc. R. Soc. Lond.* A232:159–172.
6. Brooks, J. H., and B. A. Pethica. 1964. Properties of ionized monolayers. Part 6. Film pressures for ionized spread monolayers at the heptane/water interface. *Trans. Faraday Soc.* 60:208–215.
7. Brooks, J. H., and B. A. Pethica. 1965. Comparison of spread monolayers and adsorbed monolayers at an *n*-heptane/aqueous sodium chloride interface. *Trans. Faraday Soc.* 61:571–576.
8. Yue, B. Y., C. M. Jackson, J. A. G. Taylor, J. Mingins, and B. A. Pethica. 1976. Phospholipid monolayers at non-polar oil/water interfaces. Part 1. Phase transitions in distearoyl-lecithin films at the *n*-heptane aqueous sodium chloride interface. *J. Chem. Soc. Faraday Trans. I* 72:2685–2693.
9. Pethica, B. A., J. Mingins, and J. A. G. Taylor. 1976. Phospholipid interactions in monolayers. *J. Colloid Interf. Sci.* 55:2–8.
10. Mingins, J., J. A. G. Taylor, B. A. Pethica, C. M. Jackson, B. Y. T. Yue. 1982. Phospholipid monolayers at non-polar oil/water interfaces. Part 3. Effect of chain length on phase transitions in saturated di-acyl lecithins at the *n*-heptane/aqueous sodium chloride interface. *J. Chem. Soc. Faraday Trans. I* 78:323–339.
11. Yamins, H. G., and W. A. Zisman. 1933. A new method of studying the electrical properties of monolayer films on liquids. *J. Chem. Phys.* 1:656–661.
12. Taylor, J. A. G., and J. Mingins. 1975. Properties of the non-polar oil/water interface. Part 1-Procedures for the accurate measurement of the interfacial pressure of an insoluble monolayer. *J. Chem. Soc. Faraday Trans. I* 71:1161–1171.
13. Pethica, B. A., M. M. Standish, J. Mingins, C. Smart, D. H. Iles, M. E. Feinstein, S. A. Hossain, and J. B. Pethica. 1975. The significance of Volta and compensation states and the measurement of surface potentials of monolayers. *In* Monolayers. E. D. Goddard, editor. American Chemical Society 144:123–134.
14. Gaines, G. L. Jr. 1966. Insoluble Monolayers at Liquid-gas Interfaces. Wiley Interscience, New York.
15. Davies, J. T. 1951. The distribution of ions under a charged monolayer and a surface equation of state for charged films. *Proc. R. Soc.* A208:224–247.
16. Sehgal K. C., W. F. Pickard, and C. M. Jackson. 1979. Phospholipid monolayers at the hydrocarbon-electrolyte interface. The interrelation of film potential and film pressure. *Biochim. Biophys. Acta.* 552:11–22.
17. Standish, M. M., and B. A. Pethica. 1968. Surface pressure and surface potential study of a synthetic phospholipid at the air/water interface. *Trans. Faraday Soc.* 64:1113–1122.

18. Adam, N. K., and G. Jessop. 1926. The structure of thin films. Part VIII. Expanded films. *Proc. R. Soc.* A112:362–375.

19. Vogel, V., and D. Möbius. 1988. Local surface potentials and electric dipole moments of lipid monolayers: contributions of the water/lipid and the lipid/air interfaces. *J. Colloid Interface Sci.* 126:408–420.

20. Parsons, R. 1954. Properties of electrified interfaces. *In* Modern Aspects of Electrochemistry. No. 1. J. O'M Bockris and R. E. Conway, editors. Butterworths, London. 103–179.

21. Schulman, J. H., and E. K. Rideal. 1931. The potentials of solid, liquid condensed and double layer films. *Proc. R. Soc.* A130:284–294.

22. Rideal, E. K. 1926. An introduction to Surface Chemistry. Cambridge University Press.

23. Alexander, A. E., and J. H. Schulman. 1937. Orientation in films of long-chain esters. *Proc. R. Soc.* A161:115–217.

24. Pickard, W. F., K. C. Sehgal, and C. M. Jackson. 1979. Measurement of phospholipid monolayer surface potentials at a hydrocarbon-electrolyte interface. *Biochim. Biophys. Acta.* 552:1–10.

25. Demchak, R. J., and T. Fort, Jr. 1974. Surface dipole moments of close packed un-ionized monolayers at the air-water interface. *J. Colloid Interface Sci.* 46:191–202.